scientific data

OPEN

DATA DESCRIPTOR

A 3D dental model dataset with pre/post-orthodontic treatment for automatic tooth alignment

Shaofeng Wang[1,2,4], Changsong Lei[2,4], Yaqian Liang[2] ✉, Jun Sun[1], Xianju Xie[1] ✉, Yajie Wang[3], Feifei Zuo[3], Yuxin Bai[1], Song Li[1] & Yong-Jin Liu[2] ✉

Traditional orthodontic treatment relies on subjective estimations of orthodontists and iterative communication with technicians to achieve desired tooth alignments. This process is time-consuming, complex, and highly dependent on the orthodontist's experience. With the development of artificial intelligence, there's a growing interest in leveraging deep learning methods to achieve tooth alignment automatically. However, the absence of publicly available datasets containing pre/post-orthodontic 3D dental models has impeded the advancement of intelligent orthodontic solutions. To address this limitation, this paper proposes the first public 3D orthodontic dental dataset, comprising 1,060 pairs of pre/post-treatment dental models sourced from 435 patients. The proposed dataset encompasses 3D dental models with diverse malocclusion, e.g., tooth crowding, deep overbite, and deep overjet; and comprehensive professional annotations, including tooth segmentation labels, tooth position information, and crown landmarks. We also present technical validations for tooth alignment and orthodontic effect evaluation. The proposed dataset is expected to contribute to improving the efficiency and quality of target tooth position design in clinical orthodontic treatment utilizing deep learning methods.

Background & Summary

Malocclusion is one of the three most prevalent oral diseases globally, which may lead to other oral-related conditions such as cavities, periodontitis, temporomandibular joint disorders, loose teeth, and so on. It also impacts health overall, causing problems such as cervical spine diseases and digestive system diseases[1]. Orthodontic treatment is the only way of addressing malocclusion issues by guiding teeth into proper alignment[2].

In the traditional orthodontic treatment process, orthodontists estimated the approximate post-treatment tooth position solely based on the dental condition of patients and their personal clinical experience[3]. This reliance led to highly subjective orthodontic treatment effects. In recent years, along with the advancement of digital medical technology, invisible aligners have become increasingly common. According to surveys on the preference of regular dentists for using invisible aligners, 77.3\% of respondents in the UK and Ireland (177 out of 233)[4],65.2\% of respondents in Australia (172 out of 264)[5],and 95\% of respondents in Canada (57 out of 60)[6] reported providing invisible aligner therapy for patients with malocclusion. In the invisible orthodontic treatment, it is necessary to design the target tooth position before actual treatment, which further challenges the proficiency of orthodontists in designing orthodontic target positions. Besides, in clinical practice, dental technicians are tasked with designing the target tooth position based on the descriptions of orthodontists. As depicted in Fig. 1(a), this process typically involves multiple rounds of communication and adjustments between orthodontists and technicians, resulting in higher design costs and economic burdens for orthodontic treatment.

With the tremendous success of artificial intelligence technology in many fields[7–9], leveraging deep learning-based methods to assist the orthodontic process has attracted a lot of attention from researchers and related professionals. Designing the neural networks, e.g., convolution neural networks (CNNs) and Transformers, to predict post-orthodontic treatment target positions based on pre-treatment dental models can significantly simplify or eliminate the communication process between orthodontists and dental technicians,

[1]Capital Medical University, Beijing Stomatological Hospital, Beijing, 100069, China. [2]Tsinghua University, Department of Computer Science and Technology, Beijing, 100084, China. [3]LargeV Instrument Corporation, Ltd., Beijing, 100084, China. [4]These authors contributed equally: Shaofeng Wang, Changsong Lei. ✉e-mail: yaqianliang@tsinghua.edu.cn; dentistxxj@mail.ccmu.edu.cn; liuyongjin@tsinghua.edu.cn

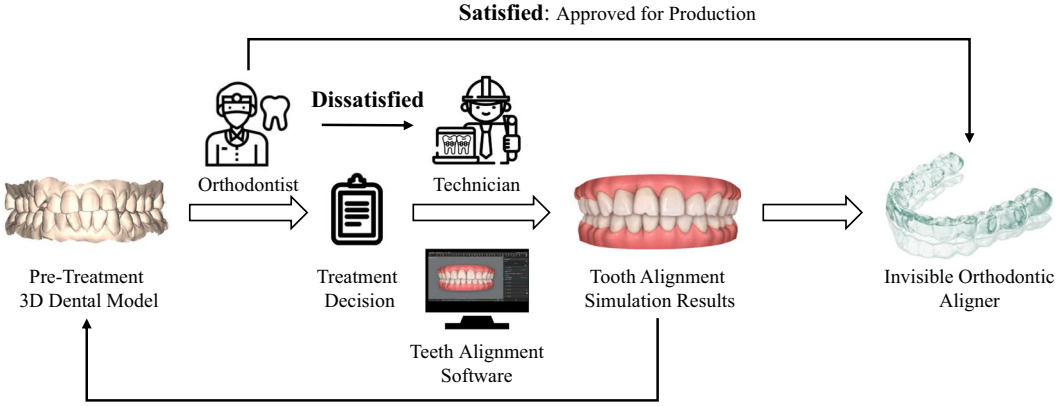

(a) Target tooth position design process in traditional orthodontic treatment process

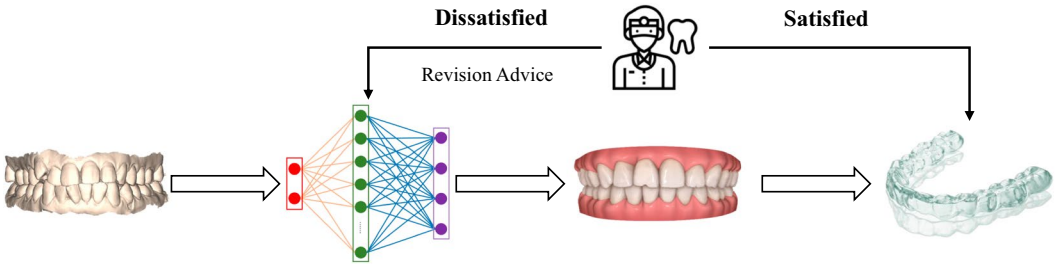

(b) Target tooth position design process based on deep learning methods

Fig. 1 Comparison between the target tooth position design process in traditional orthodontic treatment (**a**) and the target tooth position design process based on deep learning (**b**).

as shown in Fig. 1(b). Furthermore, the deep learning-based tooth alignment methods could learn the experience from existing cases, which also avoids unreasonable dental alignment designs produced by inexperienced practitioners. It could also enhance the efficiency of orthodontic diagnosis and treatment. Currently, several deep learning-based methods have been developed to achieve automatic 3D tooth alignment[10–13]. Among them, TAligNet[10], TANet[11], and PSTN[12] proposed to leverage PointNet[14] to encode the geometry of each tooth independently and generate the aligned position of each tooth with Multilayer Perceptron (MLP). In contrast, TADPM[13] proposed to generate the transformation matrix of each tooth based on the diffusion probabilistic model directly. Upon reviewing all the aforementioned methods, we find that all of them used neural networks to fit the transformation matrices of teeth. Consequently, to achieve better tooth alignment effects, the utilization of a comprehensive 3D dental model dataset encompassing various types of tooth deformities during the training phase is imperative. Nevertheless, existing methods have not disclosed the training datasets they utilize, making it impossible to determine the types of malocclusions contained within them. Therefore, it is unclear whether the existing methods can handle complex real cases in clinical orthodontic treatment.

So far, the application of artificial intelligence technology in tooth-related tasks mainly focused on tooth segmentation, and the publicly available datasets are also tooth segmentation data, such as children's dental panoramic radiographs dataset[15], CBCT dental segmentation dataset[16], and 3D dental model segmentation dataset Teeth3DS[17]. Compared to panoramic radiographs or CBCT data, 3D dental models play a more critical role in orthodontics. By providing comprehensive 3D crown morphology and spatial information, 3D dental models are indispensable for a multitude of tasks including diagnosing malocclusion, designing tooth alignment, and creating personalized orthodontic aligners. However, there is still no dataset publicly available for tooth alignment tasks that include paired (i.e., pre-orthodontic and post-orthodontic) 3D dental models. Actually, some constraints impede the establishment of orthodontic 3D dental datasets: (1) In traditional orthodontic treatments, 3D dental models were scanned from plaster models. Nevertheless, due to the long duration of orthodontic treatment, plaster models are prone to damage or loss, leading to difficulty in obtaining paired 3D dental models. (2) Performing necessary tooth segmentation and tooth position annotation on paired 3D dental models brings a huge workload. (3) Insufficient awareness of the importance of data annotation and standardized interfaces in clinical practice makes it difficult to construct professional datasets. Due to the lack of accurate and publicly available datasets containing various types of orthodontic samples, there is still a significant gap between existing methods and clinical practice.

Recently, thanks to the widespread use of intraoral scanning devices, the advantages of digital 3D dental models, such as easily storing and analyzing, have overcome the above constraints[18]. To advance the development of intelligent digital orthodontic treatment, we propose to construct a publicly accessible 3D orthodontic dental dataset, aiming to bridge the existing disparity and foster advancements in the field. After filtering

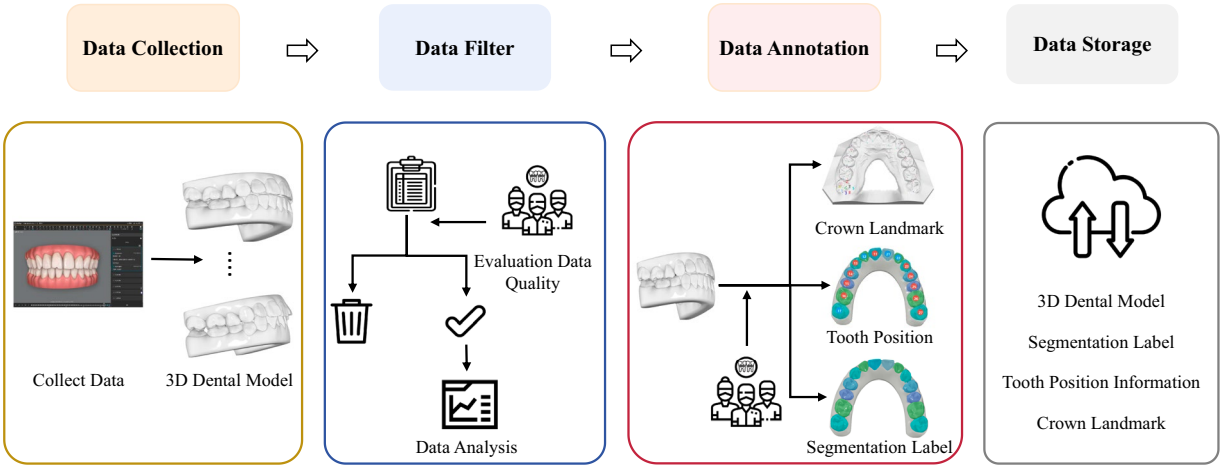

Fig. 2 The main flowchart of the dataset construction process, including the data collection, data filtering, data annotation, and data storage.

personal privacy information, we ultimately obtained 1060 pairs of high-quality dental model data, containing pre-orthodontic and post-orthodontic 3D dental models. In our dataset, there are 194 pairs of dental models in the moderate-to-severe crowding state, 352 pairs of dental models belonging to deep overbite, and 534 pairs of dental models belonging to deep overjet, which could provide a sufficient amount of challenging samples to train the tooth alignment networks.

Methods

The construction process of orthodontic dental datasets includes four main stages: data collection, data filtering, data annotation, and data storage. The main flowchart is shown in Fig. 2.

Data Collection. The proposed dataset was collected from 435 patients treated at Beijing Stomatological Hospital between February 2017 and June 2023. The study had been approved by the Ethics Committee of Beijing Stomatological Hospital Affiliated with Capital Medical University. Due to the clinical characteristics of invisible aligner treatment, most patients undergone more than one treatment phase. We treated each treatment phase as independent of others and collected the dental models pre- and post-treatment, respectively. After obtaining authorization from orthodontists and patients (or with parental consent for patients under the age of 18), we collected 1,130 pairs of pre/post-treatment 3D dental models.

We employed the iTero intraoral scanner (Align Technology, USA)[19] to acquire oral scan models (pre-orthodontic) from patients. In the preparation process, the scanning handle is fitted with a disposable scan head cover and preheated. Patients are then positioned supine and instructed to open their mouths. Subsequently, an air gun is utilized to remove saliva from the maxillofacial of the mandibular crown and adjacent concave areas. During the scanning process, we scan the crown of each tooth, starting from the distal buccal surface of the left mandibular posterior tooth and progressing sequentially towards the midline, culminating at the distal buccal surface of the right mandibular posterior tooth. The same procedure is followed for the upper dental arch. Upon completion of data collection for both upper and lower dental arches, patients are directed to occlude their teeth in maximum intercuspation. We proceed to scan the occlusion of the upper and lower jaws from the buccal side of the bilateral molars until the alignment of the upper and lower dental arches is achieved. Following intraoral scanner data processing, technicians meticulously examine the scanned 3D dental models for any deficiencies and conduct supplementary scans as deemed necessary.

The digital simulation results for target tooth alignment, referred to as post-orthodontic models, are collaboratively designed by orthodontists and dental technicians. Initially, orthodontists provide technicians with pertinent patient details, including basic information about patients, digital dental models, photographs, and chief complaints. Additionally, orthodontists outline their preliminary designs for the desired dental arch shape based on their clinical expertise. Subsequently, technicians proceed to design target tooth alignment and desired tooth movements based on the requirements of orthodontists, which undergo thorough review and approval by orthodontists, ensuring alignment with treatment objectives and clinical standards. The post-orthodontic dental models in our dataset are the models that can be used to produce invisible aligners in actual clinical orthodontics, ensuring that the orthodontic effects of ground truth in our dataset are of high quality. Therefore, by training on our dataset, the tooth alignment networks are expected to predict the ideal orthodontic effects.

Figure 3 illustrates the specific data acquisition process. In this paper, both the pre/post-orthodontic dental model data were downloaded from myitero.com (an invisible aligner company). Noted that, due to the clinical characteristics of invisible aligner treatment, most patients undergo new treatment phases during their treatments. We treated each treatment phase as independent of others, where the initial dental model at the beginning of each treatment phase was considered the pre-treatment state, and the teeth alignment designed by the technician and approved by the doctor was considered the post-treatment state. By doing this, not only

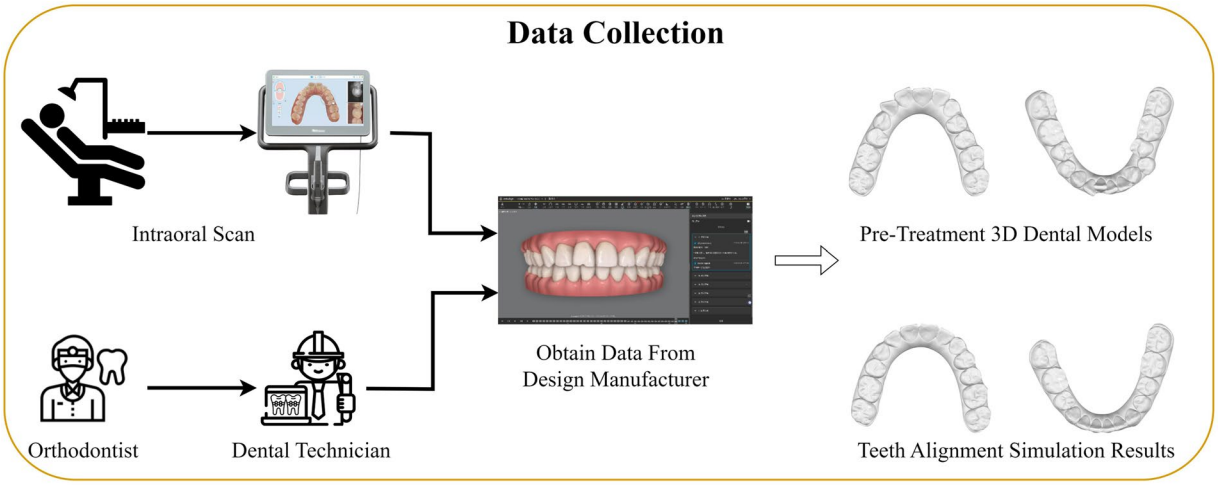

Fig. 3 The process of data collection, including performing intraoral scanning on patients and designing the target tooth alignment results.

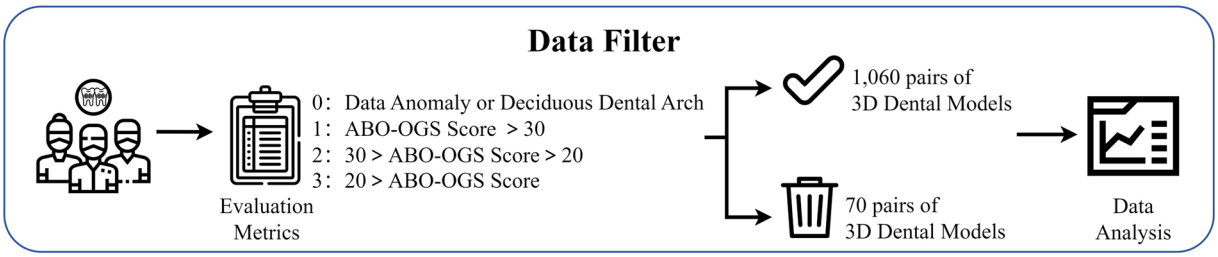

Fig. 4 The process of data filtering.

the size of our dataset could be expanded, but it could also better simulate the tooth alignment design for each treatment stage.

Data Filtering. To ensure data quality, it is essential to filter out low-quality dental models and those with unreasonable tooth alignment designs from the constructed dataset. This step enhances the reliability and accuracy of subsequent deep learning methods for predicting dental alignment outcomes.

Evaluation Metrics. Nowadays, there are two commonly used evaluation metrics, Andrews Six Elements[20] and Orthodontic ABO Scoring Standards[21]. Among them, Andrews Six Elements are proposed focusing on the characteristics of dental models without orthodontic treatments, and Orthodontic ABO Scoring Standards are proposed to evaluate the effectiveness of orthodontic treatment by measuring the distance between anatomical landmarks of the dental crown. Nevertheless, the absence of unified evaluation criteria for both pre- and post-orthodontic treatment dental models poses a significant challenge. Drawing upon existing evaluation methods, this paper proposes a novel evaluation system tailored specifically for tooth alignment tasks, which utilizes subjective scoring scales ranging from 0 to 3 to assess the quality of dental models pre- and post-orthodontic treatment. A score of 0 indicates the presence of either deciduous dental arches or abnormal data files. A score of 1 suggests that the designed post-orthodontic dental model fails to meet the Tweed's Six Keys to Normal Occlusion or exceeds a threshold of 30 in the ABO score. A score of 2 signifies that the designed post-orthodontic dental model generally adheres to Tweed's Six Keys to Normal Occlusion or falls within an ABO score range of 20-30. Lastly, a score of 3 indicates that the designed post-orthodontic dental model fully complies with Tweed's Six Keys to Normal Occlusion or achieves an ABO score below 20.

To mitigate the potential personal subjectivity bias in the evaluation process, we engaged three orthodontic specialists to collaboratively evaluate data quality. Among them, one specialist has over 20 years of clinical experience, while the other two possess more than 15 years of clinical expertise. Following training and testing in the scoring system to ensure consistency, two orthodontists evaluated all dental models independently. In cases under the consensuses between the two orthodontists, the evaluation of that data was concluded. In instances of disagreement between two orthodontists, the third orthodontist, possessing greater clinical experience, served as the arbiter to resolve disagreements. The specific procedural workflow is illustrated in Fig. 4. Subsequent to the evaluation of pre- and post-orthodontic treatment dental models, sets of data with scores below 2 were

	Dentition	Num	Dental crowding	Num	Malocclusion	Num	Overbite	Num	Overjet	Num
	Deciduous	7	Dental spacing	381	Class I	320	Normal	592	Normal	487
	Mixed	31	Mild	485	Class II	458	Deep	352	Deep	469
	Permanent	1,022	Moderate-to-severe	194	Class III	263	Negative	59	Negative	65
					Special	19	Anterior open bite	17	Edge-to-edge	39
							Edge-to-edge	40		
Total		1,060		1,060		1,060		1,060		1,060

Table 1. The statistical results of the proposed dataset from different perspectives.

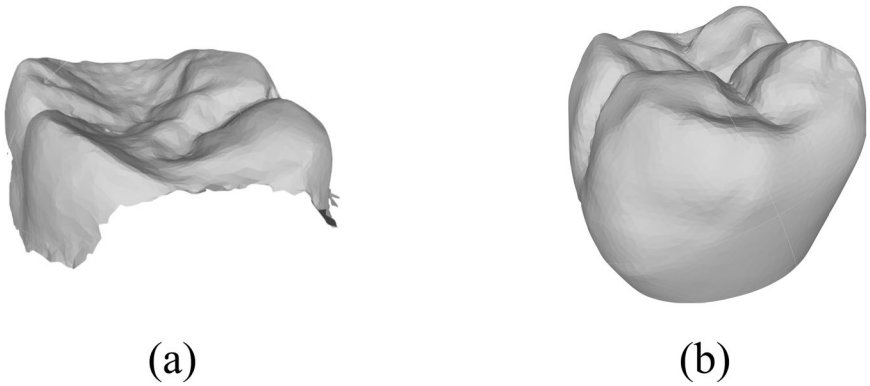

Fig. 5 Comparison of a segmented tooth between the existing dental data and our dataset.

excluded. The remaining 1,060 sets, rated 2 or 3, were deemed suitable for inclusion in the dataset, ensuring a high standard of data quality for subsequent analyses.

Data Statistics. In this section, we conduct statistical analysis on the proposed dataset, including dentition type, dental crowding degree, and occlusion characteristics, which directly influence the design of the target tooth alignment. The statistical results are illustrated in Table 1.

For dentition type, 'Deciduous' denotes only deciduous teeth are observed, 'Permanent' denotes only permanent teeth are observed, and 'Mixed' denotes that deciduous and permanent teeth are both observed. For dental crowding, 'Dental spacing' denotes the degree of crowding $< 0mm$, 'Mild' denotes $0 <$ the degree of crowding $< 4mm$, and 'Moderate-to-severe' denotes the degree of crowding $> 4mm$. For the categories of malocclusion, we classify the dataset into 'Class I', 'Class II', 'Class III', and 'Special' following the methods in[22], where 'Special' denotes the special dental models. For overbite, 'Normal' denotes that the upper anterior teeth cover 1/3 ~1/2 part of the lower anterior teeth clinical crown, 'Deep overbite' denotes that the upper anterior teeth cover more than 1/3 part of the lower anterior teeth, 'Negative overbite' denotes that the lower anterior teeth cover the upper anterior teeth and the lower anterior teeth are in front of the upper anterior teeth, 'Anterior open bite' denotes that there is space between the upper anterior teeth and the lower anterior teeth in the vertical direction, 'Edge-to-edge' denotes that the upper anterior teeth contact with the lower anterior teeth in the vertical direction. Overjet is the horizontal overlap between the upper and lower anterior teeth when the back molars bite together, where 'Normal overjet' denotes $0 <$ overjet $< 3mm$, 'Deep overjet' denotes overjet $> 3mm$, 'Negative overjet' denotes overjet $< 0mm$, 'Edge-to-edge' denotes that the upper anterior teeth are in contact with the lower anterior teeth in the horizontal direction.

Data Annotation. The data annotation is divided into three main parts: (1) segmentation annotation of dental crowns, (2) numbering annotation of tooth position, and (3) anatomical landmarks annotation on dental crowns. Given that both the annotation of tooth position and anatomical landmarks depend on the segmentation labels of dental crowns, we initiate the process by performing segmentation annotation of dental crowns, followed by the annotation of tooth position and anatomical landmarks. The specific annotation details are as follows.

Segmentation Labels Annotation of Dental Crowns. The segmentation annotation of dental crowns involves partitioning the entire dental arch into multiple single-tooth models. Traditionally, the segmentation of dental arch heavily relied on manual annotation, which was time-consuming. Besides, due to the lack of information about adjacent surfaces in the contact area, the segmented dental crowns often exhibited incompleteness, as depicted in Fig. 5(a), resulting in inaccurate data in tooth alignment tasks. In contrast, the iTero intraoral scanner employed in this paper automatically segments teeth and gingiva, followed by the filling of adjacent surfaces between teeth and the generation of virtual gingiva information simulating the natural human oral environment. This process guarantees the integrity of the proximal surface in the contact area, as illustrated in Figure 5(b).

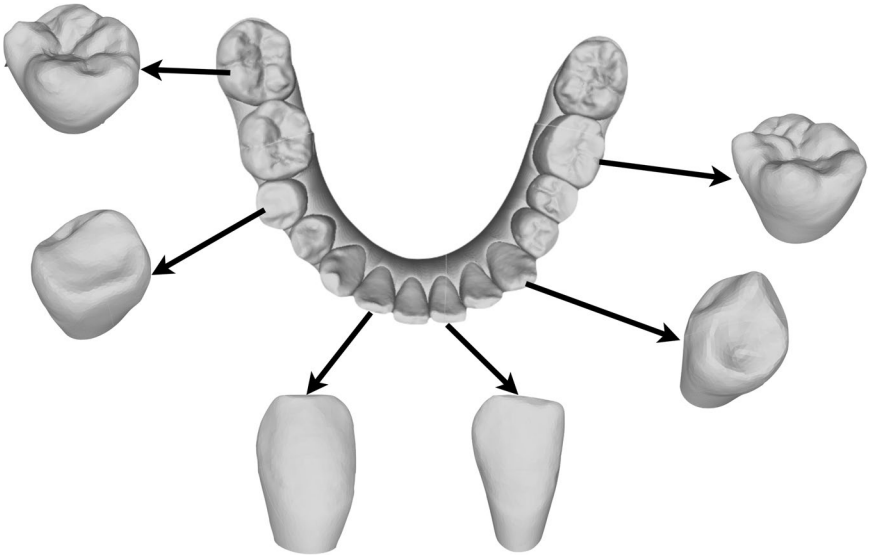

Fig. 6 An example of dental crown segmentation in our dataset.

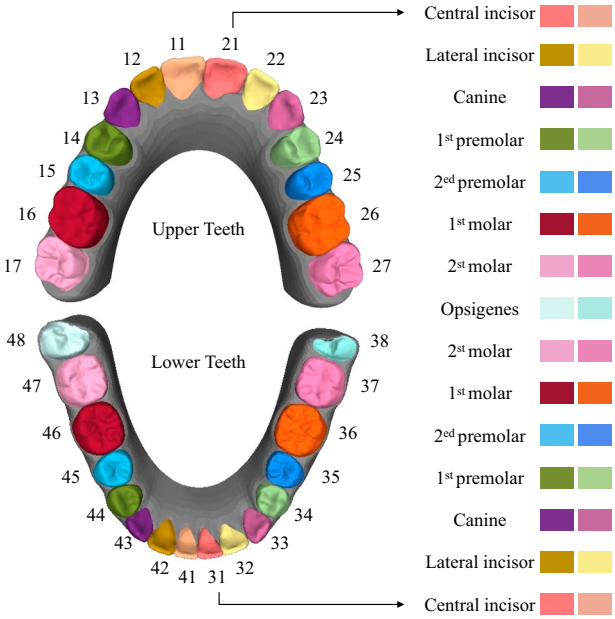

Fig. 7 The FDI tooth numbering system.

Such a distinctive data structure substantially decreases the burden of segmentation annotation and maintains the consistency of crown shape pre- and post-orthodontic treatment. Moreover, it offers a higher-quality data format conducive to automatic tooth alignment with deep learning.

In practical data processing, we used SolidWorks software to separate and extract individual dental crowns and gingiva information in closed STL format, as depicted in Fig. 6. To facilitate the annotation of segmentation labels, we developed the *Fusion Model Maker* software, which can input automatic segmentation results and allow for manual adjustments. Currently, *Fusion Model Maker* is publicly available commercially. Researchers interested in obtaining it can purchase the software from *LargeV Instrument Corporation*. Additional details are available in the Supplementary Information. To ensure the quality of the split data, we enlisted three orthodontists with over 5 years of clinical experience to preview and correct the segmented data using the *Fusion Model Maker*. They manually assessed whether the automatically segmented dental crowns conformed to clinical knowledge and examined potential disparities in the morphology of dental models pre- and post-orthodontic. The results indicate that all segmented dental crowns meet clinical standards and are suitable for tooth alignment prediction.

No.	1	2	3	4	5	6	7	Total
Kappa	0.991	0.984	0.978	0.956	0.949	0.956	0.976	0.967

Table 2. The kappa value of the tooth position numbering annotation.

Numbering Annotation of Tooth Position. In dentistry, to facilitate recording and distinguishing the positions of teeth, dentists developed the Federation Dentaire Internationale (FDI) numbering system[23], which annotates the positions of teeth based on the locations and anatomical characteristics of dental crowns. Regardless of the variation in the number of teeth present in the dentition, the tooth position numbers should remain consistent. The label settings are outlined in Fig. 7.

To enhance the efficiency of tooth position annotation, we extracted 2D occlusal view images for each single-arch model and employed the web-based annotation tool *Label Studio*[24] for image annotation and data sharing. In practice, each dental arch was independently annotated by five randomly assigned doctors, who marked the tooth number at the center of each crown. Since the entire dental arch can be divided into four quadrants, doctors labeled teeth from 1 to 7 within each quadrant. To assess the consistency of the tooth numbers annotated by different orthodontists, we calculate the kappa values for tooth labels at each position and the kappa values for tooth labels in the entire dental models, where the results are presented in Table 2. The kappa value for the entire dataset is 0.967, which is clinically acceptable. Besides, the labeling discrepancies were reviewed and corrected by the orthodontists with over 15 years of clinical experience, referring to the corresponding clinical cases. Subsequently, the labels in the 2D images were translated into 3D models by integrating tooth crown segmentation and tooth position. In cases of disparities in tooth position annotation, adjustments were made by referencing the tooth extraction decisions outlined in the actual orthodontic plan. The annotation process is illustrated in Fig. 8.

Anatomical Landmarks Annotation of Dental Crowns. Anatomical landmarks are critical factors in evaluating occlusion and the effect of orthodontics treatment. In the proposed dataset, we also provide the anatomical landmarks annotation of dental crowns, where the landmarks of each tooth are outlined in Table 3. We also illustrate the landmarks on the dental model in Fig. 9.

As there is currently no open-source annotation tool specifically designed for annotating the anatomical landmarks on digital dental models, we developed a PC software, called *Fusion Analyser*[25], to accelerate the annotation process. The Fusion Analyser is now publicly available for download (https://www.fusionalign.cn/fusionanalyser/). It facilitates easy adjustment of anatomical landmark positions and can automatically calculate various measurement indicators. For further details, please refer to the Supplementary Information. We invited 5 orthodontists with over 8 years of clinical experience to cross-annotate the anatomical landmarks of the dental crowns. For each dental model, two of the five doctors trained in using the software were randomly assigned to perform data annotation independently. A collective discussion was conducted if the error between the two annotation results exceeded $2mm$. If the error was within $2mm$, the average position of the two annotation results would be taken as the final annotation result. During the initial labeling process, the average error was $0.143mm$, well within the clinically acceptable range. The annotation workflow is illustrated in Fig. 10.

Data Privacy. To protect patient privacy, the proposed dataset has undergone an ethical review from the Ethics Committee of Beijing Stomatological Hospital Affiliated with Capital Medical University (Approval No. CMUSH-IRB-KJ-PJ-2024-02). The Ethics Committee of Beijing Stomatological Hospital has already ensured the confidentiality of personal information in the proposed dataset, and obtained consent from adult patients and the guardians of underage patients (parental consent was obtained for those under the age of 18) to include their personal data in the study, and approved the clinical dataset for study and sharing. Participants (adult patients and the guardians of underage patients) were informed about the purpose and procedure of data collection, the rights and welfare of the participants, potential risks, and the privacy protection protocol. Participants consented that the 3D dental models obtained during this study will be used for academic research and published in academic journals or books. During the data collection, we anonymized the data by replacing patient names with numeric identifiers based on the download sequence and removing data that could reveal identifiable patient private information. To guarantee the removal of all identifiable patient information, a panel of four members, including orthodontists and technicians, have conducted a cross-validation of the dataset.

Data Records

The proposed orthodontic dental dataset is available on *Zenodo*[26] (https://zenodo.org/records/11392406) upon request. The link will always work. Interested researchers are invited to submit an access request via *Zenodo*. In addition, applicants are required to adhere to the hospital's regulation policies and sign a *Data Use Agreement (DUA)*, which can be obtained at https://github.com/lcshhh/TADPM/blob/main/Data-Use-Agreement.pdf. The signed DUA should be emailed to liuyongjin@tsinghua.edu.cn. In the application email, the applicants are also required to provide basic information, including their name, affiliation, and a detailed explanation of the purpose for which the dataset is being requested. After receiving our approval emails, applicants will be granted access to download the dataset directly from *Zenodo*.

The proposed dataset contains the 3D dental models, segmentation labels, tooth position annotations, anatomical landmark annotations, and malocclusion categories. Due to the complexity of the landmark annotation process, we only provide anatomical landmark annotations for 200 pairs of representative dental models with various types of malocclusion.

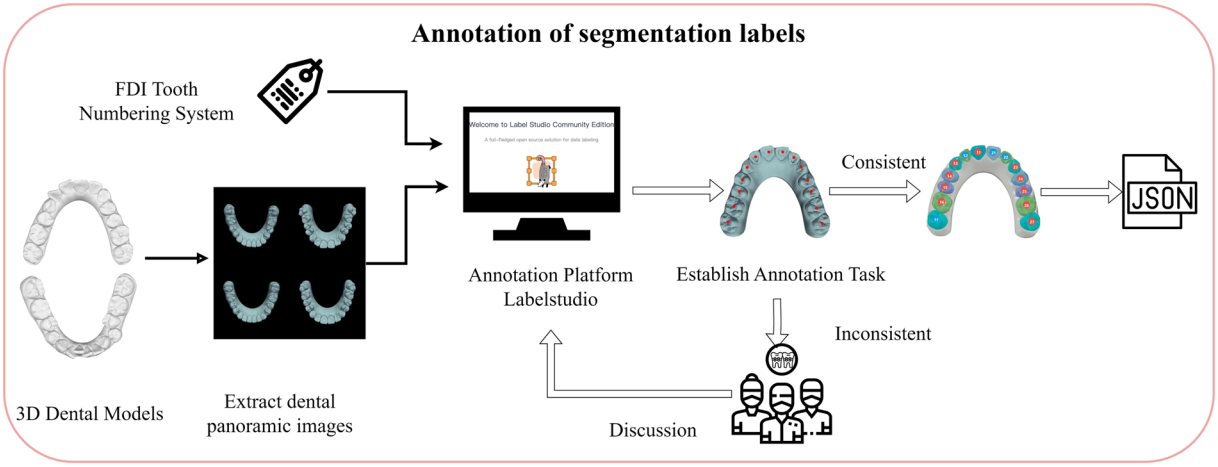

Fig. 8 The process of annotating tooth segmentation labels and tooth position numbers.

Upper														
	17	**16**	**15**	**14**	**13**	**12**	**11**	**21**	**22**	**23**	**24**	**25**	**26**	**27**
Pt0	MC	MC	BC	BC	CT	I	I	I	I	CT	BC	BC	MC	MC
Pt2	M	M	M	M	M	M	M	M	M	M	M	M	M	M
Pt3	D	D	D	D	D	D	D	D	D	D	D	D	D	D
Pt6	C	C	C	C							C	C	C	C
Lower														
	47	46	45	44	43	42	41	31	32	33	34	35	36	37
Pt0					CT	I	I	I	I	CT				
Pt2	M	M	M	M	M	M	M	M	M	M	M	M	M	M
Pt3	D	D	D	D	D	D	D	D	D	D	D	D	D	D
Pt6	C	C	C	C							C	C	C	C
Pt7	BG	BG											BG	BG

Table 3. The anatomical landmarks of teeth in upper and lower arches, where 'MC' denotes the mesiobuccal cusp tip, 'BC' denotes the buccal cusp tip, 'CT' denotes the cusp tip, 'I' denotes the incisal point, 'M' denotes the mesial contact point, 'D' denotes the distal contact point, 'C' denotes the central fossa of the tooth, and 'BG' denotes the buccal groove point.

(1) Complete dataset. The compressed file "Orthodontic_dental_dataset.rar" contains the 3D dental models and segmentation annotations. The file tree is as follows:

```
|—0001
|   |—final
|   |   |—L_Final.stl
|   |   |—L_Final.json
|   |   |—U_Final.stl
|   |   |—U_Final.json
|   |—ori
|   |   |—L_Ori.stl
|   |   |—L_Ori.json
|   |   |—U_Ori.stl
|   |   |—U_Ori.json
|—0002
|   |.....
```

- "L_Ori.stl" and "L_Final.stl" denote the dental mesh models pre- and post-orthodontic treatment of the lower jaw, respectively. And "U_Ori.stl" and "U_Final.stl" denote the dental mesh models pre- and post-orthodontic treatment of the upper jaw, respectively. The STL files in our dataset are in binary format, which can be processed by Trimesh[27], mainly including vertex and face information.
- "L_Ori.json", "L_Final.json", "U_Ori.json", and "U_Final.json" contain the segmentation annotations and tooth position annotations. The meaning of each field in "L_Ori.json" is as follows:

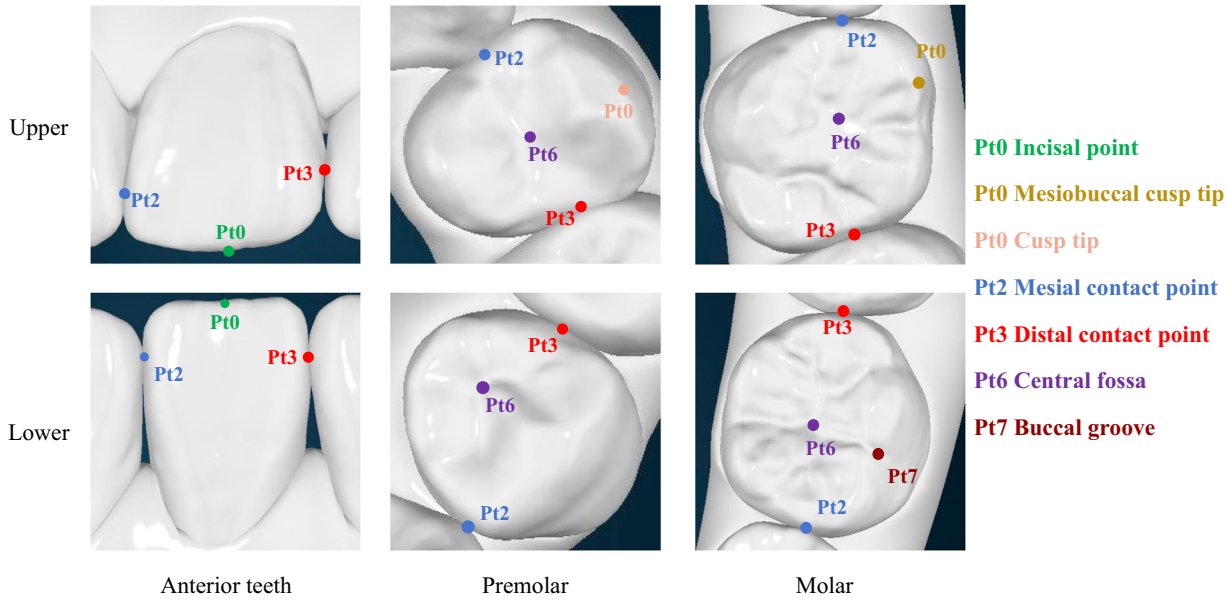

Fig. 9 The illustration of anatomical landmarks on the dental crowns.

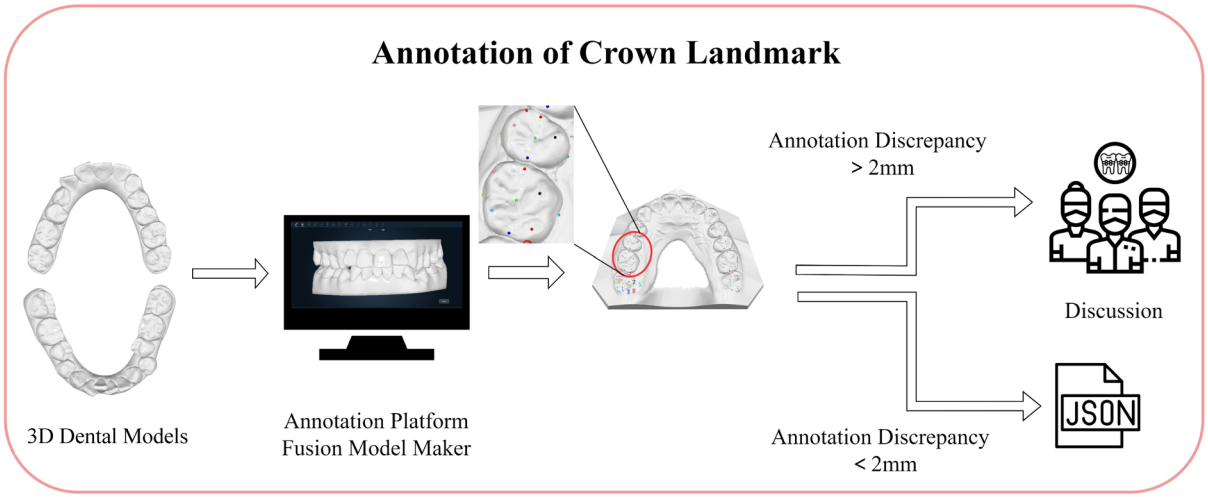

Fig. 10 The process of annotating landmarks of the dental crown.

{

"landmarks": null,

"segmentation": {

"48": {"vertices": [[25.1125, 21.2252, -1.2073], ..., [30.0578, 19.8349, -0.0504]]},

...

"38": {"vertices": [[-21.7643, 20.1912, 0.0573],..., [-26.4578, 21.0449, -0.2892]]} },

"version": "1.0.0.1"

}.

Data formats of "U_Ori.json", "L_Final.json", and "U_Final.json" are the same. Among them, "segmentation" denotes the coordinates of vertices contained in the *i*-th tooth. The order of tooth position numbers in the upper

jaw is “28 27 26 ... 21 11 12 13 ... 18”, while the order in the lower jaw is “48 47 46 ... 41 31 32 33 ... 38”. For tooth extraction cases, some teeth may be missing, and the coordinates of vertices will skip that tooth directly.

After obtaining the annotated information for segmentation labels and tooth position annotations in the dataset, we divided the data into training and test sets with a ratio of 3:1. The specific data partitioning method for test and training sets is shown in “train-test-split.txt”.

(2) Anatomical landmarks of dental crowns. We provide anatomical landmarks for 200 representative dental models in a separate folder called “Landmark_annotation.rar”. The file tree is as follows:

```
|—0001
|   |—final
|   |   |—L_Final_landmarks.json
|   |   |—U_Final_landmarks.json
|   |—ori
|   |   |—L_Ori_landmarks.json
|   |   |—U_Ori_landmarks.json
|—0002
|   |.....
```

The internal structure of the “L_Final_landmarks.json” is as follows:

- {

  “landmarks”:[

  {“jaw”: “lower”},

  {“31”:{

  “Pt0”: [-9.2395, -25.5967, -2.7286],

  “Pt2”: [-7.4205, -26.1222, -2.4053],

  “Pt3”: [-11.7712, -24.6324, -2.0932]}},

  .....

  {“47”:{

  “Pt2”: [21.5936, 4.5456, 0.4643],

  “Pt3”: [24.2688, 16.0929, 0.3872],

  “Pt6”: [22.7777, 10.1278, 0.5251],

  “Pt7”: [21.8532, -2.3854, -0.6668] }}],

  “segmentation”: {... },

  “version”: “1.0.0.1”

  }

Among them, “landmarks” contains the coordinates of anatomical landmarks on the dental models, where the meanings of “Pt0”, “Pt2”, “Pt3”, “Pt6” and “Pt7” can be found in Table 3.

(3) Category labels. As shown in Table 1, we classify the proposed dataset according to the degree of dental crowding, the type of malocclusion, the degree of overbite, the degree of overjet, and the dentition type. It is noted that the above classification methods are not independent of each other, which means there may be both dental crowding and deep overbite problems in a single dental model. Therefore, we classify the entire dataset 5 times from different perspectives, and the indexes of dental models included in each class are listed in the corresponding “txt” file.

- “Dentition.txt” contains the indexes of “Deciduous” dental models, “Mixed” dental models, and “Permanent” dental models. The specific format is as follows:

  “Deciduous”: {0015, 0133, 0172, ...},

  “Mixed”: {0014, 0022, 0026, ...},

  “Permanent”: {0001, 0002, 0003, ...}
- “Crowding.txt” contains the indexes of dental models with “Crowding_below_4”, “Crowding_above_4-”, and “Dental_spacing-”.
- “Malocclusion.txt” contains the indexes of dental models in “ClassI”, “ClassII”, “ClassIII”, and “Special”.
- “Overbite.txt” contains the indexes of dental models in “Normal_overbite”, “Deep_overbite”, “Negative_overbite”, “Anterior_open_bite”, and “Edge-to-edge_bite”.
- “Overjet.txt” contains the indexes of dental models in “Deep_overjet”, “Normal_overjet”, “Negative_overjet” and “Edge-to-edge”.

Model	ADD (↓)	PA-ADD (↓)	CSA (↑)	ME_{rot} (↓)	FD_{cur} (↓)
Input	4.807	4.894	0.640	4.328	12.843
TANet	1.998	1.817	0.868	3.948	3.936
PSTN	2.034	1.841	0.864	3.964	3.914
TAligNet	2.120	1.948	0.853	3.905	3.877
TADPM	1.765	1.548	0.879	3.929	3.523

Table 4. Comparison of tooth alignment effects obtained by state-of-the-art methods. ↓ indicates the lower the better, while ↑ indicates the higher the better. The coordinate unit for ME_{rot} is °, and the coordinate units for ADD and FD_{cur} are *mm*.

Fig. 11 Visualization of the predicted orthodontic effects obtained by the above representative methods.

Technical Validation

The global average prevalence rate of malocclusion across various ethnicities stands at 56%[28]. However, due to the long education cycle of professional orthodontists, there is a great shortage of orthodontists, leading to the growing demand for orthodontic treatment among patients is difficult to meet. With the development of artificial intelligence, assisting orthodontic treatment with deep learning methods has become a prominent research area in dentistry. To demonstrate the practical utility of the proposed orthodontic dental dataset, we provide two technical validation tasks, including tooth alignment and orthodontic effect evaluation.

Model	ADD (↓)	PA-ADD (↓)	CSA (↑)	ME_{rot} (↓)	FD_{cur} (↓)
TANet	1.805	1.699	0.866	3.896	3.793
PSTN	1.891	1.766	0.863	3.929	3.817
TAligNet	1.831	1.725	0.870	3.875	3.722
TADPM	1.410	1.307	0.889	3.802	3.284

Table 5. Comparison of tooth alignment effects for samples with tooth crowding. ↓ indicates the lower the better, while ↑ indicates the higher the better.

Model	ADD (↓)	PA-ADD (↓)	CSA (↑)	ME_{rot} (↓)	FD_{cur} (↓)
TANet	1.770	1.659	0.862	3.973	3.701
PSTN	1.833	1.715	0.867	4.028	3.766
TAligNet	1.723	1.628	0.875	3.992	3.620
TADPM	1.429	1.283	0.879	3.951	3.362

Table 6. Comparison of tooth alignment effects for samples with deep overjet. ↓ indicates the lower the better, while ↑ indicates the higher the better.

Model	ADD (↓)	PA-ADD (↓)	CSA (↑)	ME_{rot} (↓)	FD_{cur} (↓)
TANet	1.804	1.697	0.868	3.911	3.579
PSTN	1.893	1.741	0.864	3.929	3.754
TAligNet	1.827	1.716	0.873	3.903	3.615
TADPM	1.502	1.380	0.881	3.895	3.405

Table 7. Comparison of tooth alignment effects for samples with deep overbite. ↓ indicates the lower the better, while ↑ indicates the higher the better.

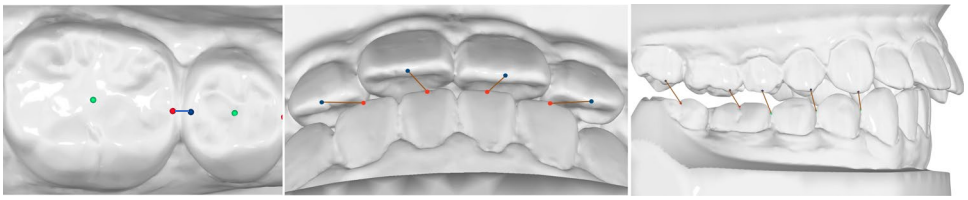

(a) Alignment (b) Anterior occlusion (c) Posterior occlusion

Fig. 12 The illustration of the proposed occlusion evaluation metrics.

Tooth Alignment Validation. In this subsection, we leverage four state-of-the-art deep learning-based tooth alignment methods to conduct the experiments, i.e., TANet[11], PSTN[12], TAligNet[10], and TADPM[13]. Among them, TANet pioneered a learning-based tooth alignment approach, which employed PointNet to extract the feature of crown point clouds and utilized a graph neural network (GNN) to implement feature propagation between teeth through topological relations. Following it, PSTN and TAligNet utilized PointNet to encode the geometry of each tooth independently, and predict the transformation matrix of each tooth with MLP. TADPM proposed a tooth alignment method based on mesh models and introduces the diffusion probabilistic model to generate the transformation matrix of each tooth by gradual denoising from a random variable. It is noted that the code of TANet, PSTN, and TAligNet is not publicly available. We have reproduced them based on the descriptions in their papers.

To measure the alignment performance, we leverage 5 evaluation metrics, including ADD[29], PA-ADD, cosine similarity accuracy (CSA), mean error of rotation (ME_{rot}), and Fréchet Distance[30] (FD_{cur}). ADD represents the point-wise mean distance between the predicted dental models and ground truth, offering an intuitive measure of alignment error. PA-ADD calculates the ADD metric following rigid registration from prediction to ground truth. CSA measures the disparity between the predicted transformation matrices and the ground truth. ME_{rot} indicates the average rotation error, while FD_{cur} quantifies the Fréchet Distance between dental arch curves of prediction and ground truth.

First of all, we conduct tooth alignment experiments using the entire dataset, and the experimental results are shown in Table 4, in which 'Input' refers to the results computed using pre-orthodontic dental models and real post-orthodontic dental models (ground truth). Based on 'Input', we provide the reference ranges for the evaluation metrics used in this paper: ADD, PA-ADD, ME*rot*, and FD*cur* have reference ranges of (0, 4.807), (0, 4.894), (0, 4.328), and (0, 12.843), respectively, where smaller values indicate better performance. Conversely,

Evaluation Metric	Computing method
The alignment of teeth	Calculate the 3D distance between the adjacent mesial contact point and distal contact point of two adjacent teeth.
Occlusal relationship in anterior teeth	Calculate the 3D distance between the midpoint of the incisal end of the maxillary incisors and the midpoint of the incisal end of the mandibular incisors.
Occlusal relationship in posterior teeth	Calculate the 3D distance between the buccal cusp of the maxillary posterior teeth and the buccal cusp of the mandibular premolar or the buccal groove of the mandibular molar.

Table 8. The proposed occlusion evaluation metrics and corresponding calculation methods.

Model	Alignment (↓)	Occlusal relationship in anterior teeth (↓)	Occlusal relationship in posterior teeth (↓)
Input	56.732	21.143	6.480
Ground Truth	36.625	14.257	5.360
TANet	55.984	19.310	6.081
PSTN	55.741	20.535	6.383
TAligNet	56.085	19.568	6.148
TADPM	54.752	18.007	5.885

Table 9. Comparison of occlusion indicators in aligned dental models. ↓ indicates the lower the better.

the reference range for CSA is (0.640, 1), with a value closer to 1 indicating better performance. If the predicted orthodontic results exceed these reference ranges, it indicates that the tooth alignment algorithm is not working. According to the experimental results, our dataset obtains ADD mean value of 1.765, PA-ADD mean value of 1.548, CSA mean value of 0.879, ME_{rot} mean value of 3.929, and FD_{cur} mean value of 3.523 by TADPM, which also performs well in other networks and other metrics, showing that the proposed dataset can be well applied to train the tooth alignment neural networks. We also demonstrate several representative aligned dental models obtained by the aforementioned methods in Fig. 11, where the first two rows display results for permanent dentition, and the last two rows show results for deciduous and mixed dentitions. The tooth alignment results achieved with TADPM are notably superior to those achieved by other methods.

Subsequently, we have chosen several certain types of dental models to construct sub-datasets, including tooth crowding over 4 *mm* (194 dental models), deep overbite (352 dental models), and deep overjet (469 dental models). Then, we conduct tooth alignment experiments on these sub-datasets to verify the orthodontic effect of the above method in severe cases. The experimental results are shown in Tables. 5, 6, and 7, respectively. Compared with the results trained on the complete dataset, the results on specific types of dental models are better, indicating that the difficult samples provided by our dataset can improve the generalization and robustness of the trained neural networks.

Orthodontic effect evaluation validation. To assess occlusion and orthodontic treatment effects, various clinical evaluation systems have been developed based on dental crown anatomical landmarks, such as the ABO-OGS index[31], DI index[32], ICON index[33], and so on. However, these metrics are only applicable for evaluating pre-treatment or post-treatment dental models. In this paper, by referencing the measurement methods of the ABO-OGS index and DI index, we propose several relatively simplified occlusion evaluation metrics based on dental crown anatomical landmarks as shown in Fig. 12, which can simultaneously adapt the pre-treatment and post-treatment dental models. The computing methods of the proposed evaluation metrics are listed in Table 8.

Based on the proposed evaluation metrics, we calculate the occlusal indicators of the aligned results obtained by TANet, PSTN, TAligNet, and TADPM, as shown in Table 9. In the table, 'Input' denotes the occlusal indicators of pre-orthodontic dental models, and 'Ground Truth' denotes the occlusal indicators of the real post-orthodontic dental models. Although the alignment results predicted by several methods have improved compared to pre-orthodontic (Input), they are still far from the ground truth, especially in terms of alignment. We regard this severe gap comes from two main sources. First, existing deep learning-based automated tooth alignment methods incorporated very little orthodontic prior knowledge. Among the above methods, none of them took tooth collision, occlusion relationships between the upper and lower arches, or other critical orthodontic concerns into the training process. Consequently, despite the predicted orthodontic results appearing well-aligned, they failed to meet the stringent requirements for clinical applications. Second, the ground truths in our dataset were scanned from real patients' dental models after orthodontic treatment. Therefore, they encapsulated extensive expertise and aesthetic considerations of orthodontists, such as the incisor inclination angles, arch width, facial soft tissue profile, and so on, making predictions much more difficult with data-driven deep learning-based methods. Given these reasons, there is still great research space for designing advanced deep learning methods to achieve automatic tooth alignment.

Usage Notes

Interested researchers can download the orthodontic dental dataset from *Zenodo*[26] (https://zenodo.org/records/11392406) to conduct further studies. The proposed dataset is encouraged for academic research, including developing deep learning-based tooth segmentation networks, tooth alignment networks, and so on.

3D Dental model files in this repository are in *stl* format, and users can use any 3D render software to open them (e.g., MeshLab[34] and Blender) or utilize python programming tools to process them (e.g., Trimesh[27] and Vedo[35]). Annotation information is saved in *json* format, which can be opened by any text editor or imported into programming tools (e.g., python) for further analysis.

Besides, it is noted that in this paper, our proposed dataset does not include the automatic generation of orthodontic treatment plans (e.g., tooth extraction) prior to the prediction of tooth alignment. Instead, we use the actual clinical outcome as the ground truth and perform tooth extractions in the pre-treatment dental model as well. When utilizing this dataset for training neural networks, we recommend referring to the established extraction plan and using the dental models in the training set as the input directly, rather than allowing the network to predict which teeth need to be extracted. We hope that the published dataset will be available to more researchers and encourage more authors to publish their optimized code and models, which will contribute to the development and advancement of the field of artificial intelligence-assisted tooth alignment.

Code availability

In this part, we provide the source code of TADPM, where code for tooth alignment and orthodontic effect evaluation introduced in technical validation is available at https://github.com/lcshhh/TADPM. The source files in this repository include 3D dental model preprocessing, feature embedding, tooth alignment network, and occlusion indicators calculation. More details about the source code can be found in the *README.md* file inside the repository.

Received: 3 June 2024; Accepted: 14 November 2024;
Published online: 23 November 2024

References

1. De Ridder, L., Aleksieva, A., Willems, G., Declerck, D. & Cadenas de Llano-Pérula, M. Prevalence of orthodontic malocclusions in healthy children and adolescents: a systematic review. *International Journal of environmental research and public health* **19**, 7446 (2022).
2. Mohlin, B. *et al*. Tmd in relation to malocclusion and orthodontic treatment: a systematic review. *The Angle Orthodontist* **77**, 542–548 (2007).
3. Ke, Y., Zhu, Y. & Zhu, M. A comparison of treatment effectiveness between clear aligner and fixed appliance therapies. *BMC oral health* **19**, 1–10 (2019).
4. Meade, M. J., Weir, T., Seehra, J. & Fleming, P. S. Clear aligner therapy practice among orthodontists in the United Kingdom and the Republic of Ireland: a cross-sectional survey of the British orthodontic society membership. *J. orthodontics* **51**, 120–129 (2024).
5. Meade, M. J. & Weir, T. A cross-sectional survey of the use of clear aligners by general dentists in Australia. *Clin. Exp. Dent Res.* **10**(4), e919 (2024).
6. Miranda e Paulo, D. *et al*. Clear aligner therapy practices among orthodontists practicing in Canada. *Prog. Orthod.* **25**, 27 (2024).
7. Wu, T. *et al*. A brief overview of chatgpt: The history, status quo and potential future development. *IEEE/CAA Journal of Automatica Sinica* **10**, 1122–1136 (2023).
8. Subhadra, K. & Vikas, B. Neural network based intelligent system for predicting heart disease. *International Journal of Innovative Technology and Exploring Engineering* **8**, 484–487 (2019).
9. Sanil, N., Rakesh, V., Mallapur, R., Ahmed, M. R. *et al*. Deep learning techniques for obstacle detection and avoidance in driverless cars. *2020 International Conference on Artificial Intelligence and Signal Processing (AISP)*, 1–4 (IEEE, 2020).
10. Lingchen, Y. *et al*. iorthopredictor: model-guided deep prediction of teeth alignment. *ACM Trans. Graph.* 216 (2020).
11. Wei, G. *et al*. Tanet: Towards fully automatic tooth arrangement. *Eur. Conf. Comput. Vis.*, 481–497 (2020).
12. Li, X. *et al*. Malocclusion treatment planning via pointnet based spatial transformation network. *Medical Image Computing and Computer Assisted Intervention*, 105–114 (2020).
13. Lei, C. *et al*. Automatic tooth arrangement with joint features of point and mesh representations via diffusion probabilistic models. *Computer Aided Geometric Design* 102293, https://doi.org/10.1016/j.cagd.2024.102293 (2024).
14. Qi, C. R., Yi, L., Su, H. & Guibas, L. J. Pointnet++: Deep hierarchical feature learning on point sets in a metric space. *Adv. Neural Inform. Process. Syst.***30** (2017).
15. Zhang, Y. *et al*. Children's dental panoramic radiographs dataset for caries segmentation and dental disease detection. *Scientific Data* **10**, 380 (2023).
16. Cui, Z. *et al*. A fully automatic ai system for tooth and alveolar bone segmentation from cone-beam ct images. *Nature Communications* 2096 (2022).
17. Ben-Hamadou, A. *et al*. Teeth3ds: a benchmark for teeth segmentation and labeling from intra-oral 3d scans. *arXiv preprint arXiv:2210.06094* (2022).
18. Petre, A. E. *et al*. Modular digital and 3d-printed dental models with applicability in dental education. *Medicina* **59**, 116 (2023).
19. Wang, X. *et al*. Coordinate-based data analysis of the accuracy of five intraoral scanners for scanning completely dentate and partially edentulous mandibular arches. *The Journal of Prosthetic Dentistry* (2024).
20. Andrews, L. F. The 6-elements orthodontic philosophy: Treatment goals, classification, and rules for treating. *American Journal of Orthodontics and Dentofacial Orthopedics* **148**, 883–887 (2015).
21. Song, G.-Y. *et al*. Validation of the american board of orthodontics objective grading system for assessing the treatment outcomes of chinese patients. *American Journal of Orthodontics and Dentofacial Orthopedics* **144**, 391–397 (2013).
22. Juneja, M. *et al*. Oclu-net for occlusal classification of 3d dental models. *Machine Vision and Applications* **31**, 1–12 (2020).
23. Peck, S. & Peck, L. A time for change of tooth numbering systems. *Journal of dental education* **57**, 643–647 (1993).
24. Tkachenko, M., Malyuk, M., Holmanyuk, A. & Liubimov, N. Label Studio: Data labeling software Open source software available from https://github.com/heartexlabs/label-studio (2020-2022).
25. Wang, S. *et al*. Fusionanalyser: A novel measurement method and software tool for dental model analysis in orthodontics. *Measurement Science and Technology* (2024).
26. Wang, S. *et al*. A 3d dental model dataset with pre/post-orthodontic treatment for automatic tooth alignment [data set]. *Zenodo*.https://doi.org/10.5281/zenodo.11392406 (2024).
27. Dawson-Haggerty *et al*. Trimesh, https://trimesh.org/ (2019).
28. Stomatologic, S. Worldwide prevalence of malocclusion in the different stages of dentition: A systematic review and meta-analysis. *European journal of paediatric dentistry* **21**, 115 (2020).
29. Hinterstoisser, S. *et al*. Model based training, detection and pose estimation of texture-less 3d objects in heavily cluttered scenes. *Asian Conf. Comput. Vis.*, 548–562 (Springer, 2013).

30. Eiter, T. & Mannila, H. Computing discrete fréchet distance. Tech. Rep., Christian Doppler Laboratory for Expert System, TU Vienna, Austria (1994).
31. Casko, J. S. *et al*. Objective grading system for dental casts and panoramic radiographs. *American Journal of Orthodontics and Dentofacial Orthopedics* **114**, 589–599 (1998).
32. Cangialosi, T. J. *et al*. The abo discrepancy index: a measure of case complexity. *American Journal of Orthodontics and Dentofacial Orthopedics* **125**, 270–278 (2004).
33. Savastano, N. J. Jr., Firestone, A. R., Beck, F. M. & Vig, K. W. Validation of the complexity and treatment outcome components of the index of complexity, outcome, and need (icon). *American journal of orthodontics and dentofacial orthopedics* **124**, 244–248 (2003).
34. Cignoni, P. *et al*. MeshLab: an Open-Source Mesh Processing Tool. *Eurographics Italian Chapter Conference*, https://doi.org/10.2312/LocalChapterEvents/ItalChap/ItalianChapConf2008/129-136 (2008).
35. Musy, M. *et al*. Vedo, a python module for scientific analysis and visualization of 3d objects and point clouds, https://doi.org/10.5281/zenodo.4287635 (2021).

Acknowledgements

This work was supported by Beijing Natural Science Foundation (L222008) and Beijing Hospitals Authority Clinical Medicine Development of Special Funding Support (ZLRK202330), Beijing Natural Science Foundation (L232028), and China Postdoctoral Science Foundation (2024M751691).

Author contributions

S.F.W., J.S., Y.J.W, F.F.Z., S.L., and Y.X.B. collected data and processed data. Y.Q.L. and S.F.W. prepared the first draft of the manuscript. C.S.L. conducted technical validation. Y.J.L. originated the concept for this study and supervised the experiment design. All authors reviewed the manuscript.

Competing interests

The authors declare no competing interests.

Additional information

Supplementary information The online version contains supplementary material available at https://doi.org/10.1038/s41597-024-04138-7.

Correspondence and requests for materials should be addressed to Y.L., X.X. or Y.-J.L.